https://doi.org/10.2352/ISSN.2169-4451.2017.32.170

Inkjet Printing onto Patterned Substrates

Beth K. Kazmierski[1], Lisong Yang[1], Emma L. Talbot[1], Colin D. Bain[1], Li Wei Tan[2], Dan Walker[2]; [1] Durham University, Department of Chemistry, Durham, DH1 3LE, United Kingdom; [2]Merck Chemicals, Chilworth, Southampton, SO16 7QD, United Kingdom

Abstract

The drying of picolitre droplets printed onto patterned substrates has been imaged. Organic solvents were printed in a drop-on-demand format into 200 μm × 200 μm square wells surrounded by walls of polymer resist which were 1.5 μm high and 20 μm wide. Particle tracking velocimetry (PTV) data revealed the velocity and direction of flows during drying, which could be understood in terms of differential rates of evaporation across the drop. Alongside PTV, interferometry was used to observe the profile of the drop during drying. The measurements revealed that variations in the evaporation rates across the drop were not the only cause of uneven deposits when printing onto patterned substrates. More important was the capillary suction caused by negative curvature in the drop once the level of the fluid dropped below the tops of the walls defining the wells, if the drying droplet was pinned at the tops of the walls. For fast evaporating drops, we observed the formation of a dimple in the centre of the well towards the end of drying.

Introduction

It is well known that drops containing solutes or particulate suspensions do not dry on flat substrates to give even deposits. Enhanced evaporation at the contact line leads to capillary flows within drops which leave behind ring-like deposits. This is often referred to as the coffee-ring effect and is undesirable in inkjet printing as it reduces the quality of printed images and limits resolution [1,2,3]. In certain cases, the coffee-ring effect can even hamper the performance of printed products (eg in printed displays or printed electrical circuits) [4,5,6,7]. There are a number of reports in the literature of methods for mitigating ring stains; however they are often limited to specific formulations or applications [8,9,10,11,12].

The published literature on droplet drying usually refers to isolated drops in the vapour phase or sessile drops on flat, uniform substrates. An unconstrained drop on a flat substrate adopts the shape of a spherical cap and the drying problem has azimuthal symmetry. In many applications, one wants to define exactly where the ink ends up on the substrate and/or to isolate certain areas of fluid from others [6,7,13]. When this is the case, drops are printed into wells that are bounded by physical and/or chemical barriers. The presence of walls breaks the cylindrical symmetry of the drying problem as well as modifying the evaporation patterns and boundary conditions of the contact line. All of these factors influence the capillary flows in drying drops, and as a consequence strategies which give uniform deposits on flat substrates are not necessarily directly applicable to patterned substrates. In order to produce even deposits on patterned substrates it is first necessary to understand what causes the deposit to become uneven in the first place.

In this paper we present results on a number of different organic solvents drying in square wells. Our goal was to understand how these solvents dry in patterned substrates and how this leads to uneven deposits. This gives us the basis on which to build to even out deposits from drops drying in square wells.

Experimental

The drying of six organic solvents was investigated: anisole (ReagentPlus, 99%), methyl anisole (99%), dimethyl anisole (99%), methyl benzoate (99%), mesitylene (98%) and o-xylene (99%). All solvents were supplied by Sigma Aldrich and used as supplied. Two experimental techniques were used to investigate the drying of drops in patterned substrates; particle tracking velocimetry (PTV) and interferometry.

Solutions were ejected from a piezo-electric single nozzle print head (Microfab, MJ-ABP-01) with an orifice diameter of 50 μm. The print head was actuated with a symmetrical bipolar waveform with the voltage set to give a single drop per pulse. Drops were deposited onto substrates provided by Merck Chemicals, which contained an array of 200 μm × 200 μm square wells surrounded by walls of polymer resist 1.5 μm high and 20 μm wide. Substrates were cleaned in an ultrasonic bath in IPA for 2 × 15 minutes, with a change of IPA, followed by 1 × 15 minutes in ultrahigh purity water. Substrates were then blown dry with argon before being dried in an oven at 230 °C for 2 hours.

For PTV measurements, the fluid was seeded with 500-nm silica beads (Kisker-biotech, fluo-green beads) as tracer particles. Drying drops were deposited onto the substrate, which was in the focal plane of an objective lens (Nikon, TU Plan ELWD, 50× magnification, numerical aperture 0.6). The lens was mounted directly underneath the substrate. Illumination came from a blue LED (Thorlabs, 1000 mA, 470 nm) which sat above the substrate at an oblique angle so only forward scattered light from the particles could be seen. Drying was recorded with a high-speed camera (Photron, fastcam SA4) at rates between 125 and 1000 fps, so particle movement could be tracked frame by frame. Particle tracks were analysed to give the velocity and direction of particle movement, which was assumed to follow the fluid flow.

For interferometry measurements the drying drops were illuminated from below through a beam splitter. An LED (Thorlabs, 1000 mA, 470 nm) was used. The substrate/drop and the drop/air interfaces provided different reflective surfaces, giving two reflected beams from the illumination light which recombined before reaching the camera to give an interference pattern in the final images. As reflections from the substrate were constant, any changes in the interference patterns seen could be attributed to the changing profile of the drying drops.

Analysis of the images began at the end of drying and counted backwards through the frames to build up a picture of how the profile of the drop changed as drying progressed. Each fringe (bright to bright) represented a 155 nm change in thickness and the coherence length of the LED was of the order of 10 μm. The sharpness of the images decreased as the film thickness increased owing to the finite coherence length of the

LED and led to the miscounting of some fringes in the early stages of drying. Therefore the plots of film profile appear to be more "noisy" for early film profiles. The region very close to the walls was excluded from analysis: Here the fringes were very close spaced and superimposed on scattering from the walls themselves, making interferometric analysis unreliable. Consequently the height plots in figures 7 and 10 do not extend up to the edges of the wells.

Results and Discussion

The PTV measurements showed that in the initial stages of drying, flows were radially outwards towards the contact line (figure 1) with the fastest particle movement at the edges and in the corners of the wells. Figure 2 shows the spatially binned average velocity vectors. The pattern of particle movement suggested evaporation was fastest at the edges of the drop and slowest across the apex, so capillary flows came from the centre of the drop towards the contact line to counteract the relative loss of fluid, very much like a drop with an unconstrained contact line drying on a flat substrate.

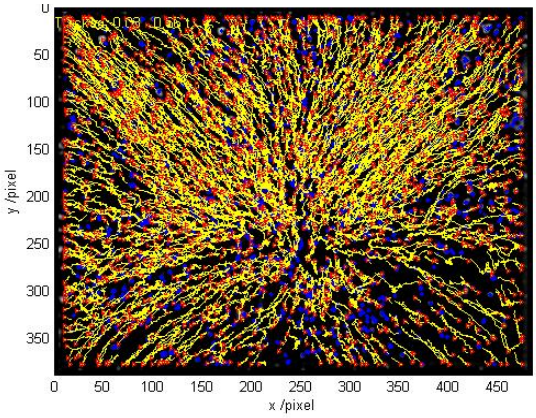

Figure 1. *Tracks for the early stages of drying (from the end of spreading to halfway through drying) for a methyl anisole drop in the square wells. Images were recorded at 1000 fps. The blue dots show particles which were stationary throughout drying, red dots are the end of movement and the yellow tails show the traiectorv of movement.*

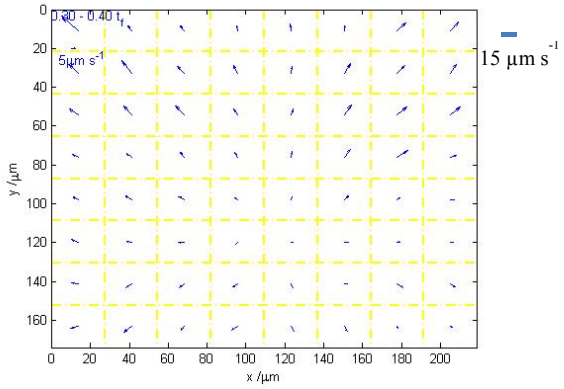

Figure 2*. Vectors showing the average speed and movement of the particles within each spatial bin between 0.3 and 0.4 of the drying time where the total drying time is 1. The flows which correlate to this movement are seen in figure 1.*

Interferometry showed that in these early stages of drying, the surface of the drop was well above the walls in the form of a quasi-spherical cap (figure 3), giving a profile similar to that of a spherical cap on a flat substrate, explaining the radial flows (figure 4). All solvents imaged through PTV (anisole, methyl anisole and methyl benzoate) showed the same initial radial flow with the only difference from solvent to solvent being the speed of particle movement, which was directly correlated to the speed of drying of the solvent.

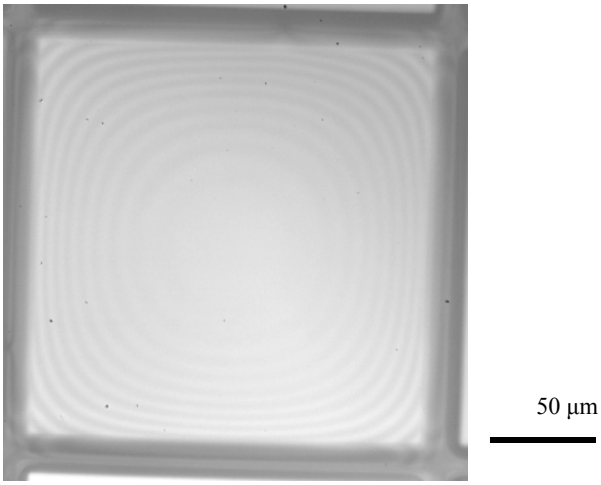

Figure 3. *An interferometry image showing the printed drop in the square well. At this point the drop is sitting above the level of the walls in the form of a quasi-spherical cap.*

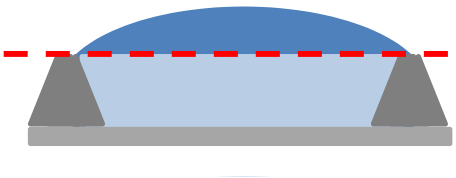

Figure 4*. A schematic showing a drop in the early stages of drying. The light and dark blue fluid represent the same drop, different colours have been used to distinguish areas above and below the top of the walls. Above the red line the drop is a quasi-spherical cap.*

In the later stages of drying (roughly the last third of the drying time), the pattern of particle movement in the drops changed. Movement began to concentrate around the edges of the wells towards the corners and there was little movement from the centre (figure 5). Again the pattern of particle movement was the same for all solvents imaged with the only differences being the speed of movement. Interferometry showed that as the drop dried past the point where it was flat and level with the bank walls the profile of the film depended on the drying rate of the drops.

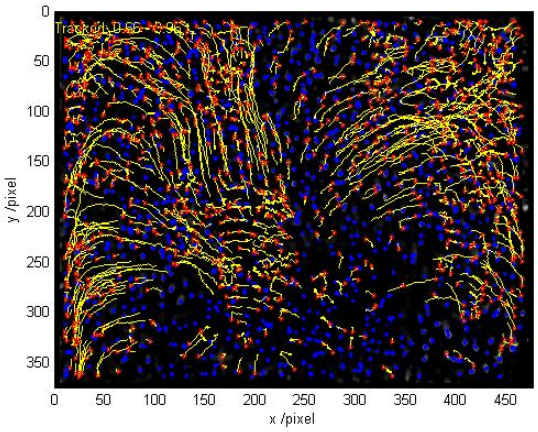

Figure 5. *Particle tracks for the later stages (from two-thirds of the way through drying until the drop was dry) of drying of the methyl anisole drop in the wells.*

For the slower drying solvents with drying times between 10 and 60 s (mesitylene, dimethyl anisole, methyl benzoate) the drop remained pinned at the tops of the walls and took on the shape of an inverted spherical cap (figure 7). In the very late stages of drying the central region of the fluid flattened out to leave behind a flat central region which then curved very steeply upwards at the edges of the wells to the tops of the walls (figures 6 and 7). In the case of these slow drying solvents the central region of the drop dried before the edges and a U- shaped final film profile was seen.

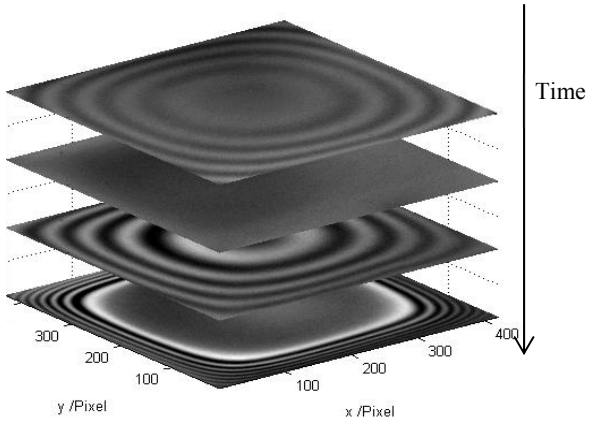

Figure 6. *A slice plot showing the changing interferometry patterns from a slow drying dimethyl anisole drop. Images were recorded at 500 fps. The top image is at the beginning of drying and the bottom image near the end of drying.*

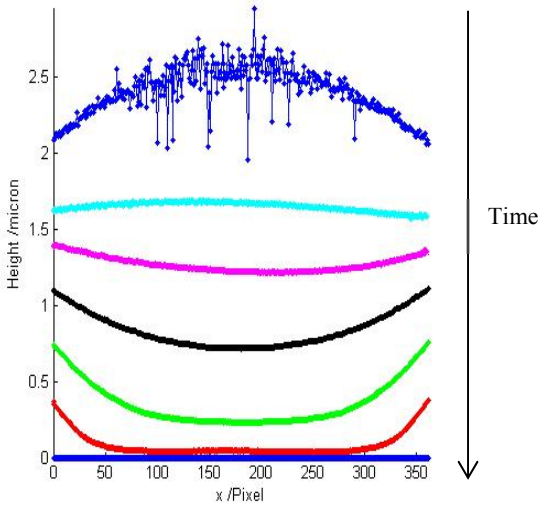

Figure 7*. The changing profile of a drying dimethyl anisole drop with a U-shaped final film profile. Time progresses from the top of the plot to the bottom. Total drying time was 45 s and the curves are equally spaced in time.*

The profile in the later stages of drying provided an explanation for the PTV tracks from the end of drying. Flows were only around the edges of the wells as this was the only region of the well containing fluid deep enough for the particles to flow through. The concentration of movement towards the corners was a result of curvature in the drying film (figure 8). The curvature in the film from the bottom of the wells up to the wall tops, as the drop pinned there, caused a negative Laplace pressure which pulled the fluid in the film towards the walls. The fluid in the corners was curved in two directions giving a greater negative pressure than along the edges in which the fluid was only curved in one direction, so it travelled along the edges of the walls towards the corners.

Figure 8. *A schematic showing the curvature in the drop as it dried down past the level of the walls and remained pinned at the top, along with the resulting capillary suction to the edges of the banks.*

For the faster drying solvents with drying times less than 10 s (methyl anisole, anisole, o-xylene) the drop also remained pinned at the tops of the walls and initially took on the profile of an inverted spherical cap. However, as the drying progressed, a raised region formed in the centre of the wells whereby thinning became fastest in the intermediate regions and slower in the centre of the wells. This pattern is similar to the "dimple" formed when a liquid drop lands on a liquid surface or when two emulsion drops collide [14] and will henceforth be referred to as dimpling of the film. Therefore the thickest fluid regions were in the centre and at the edges, with the thinnest regions in the intermediate areas of the wells (figures 9 and 10). In the case of these fast drying solvents, the central region dried either at the same rate as or faster than the fluid at the edges and a W- shaped film profile was seen.

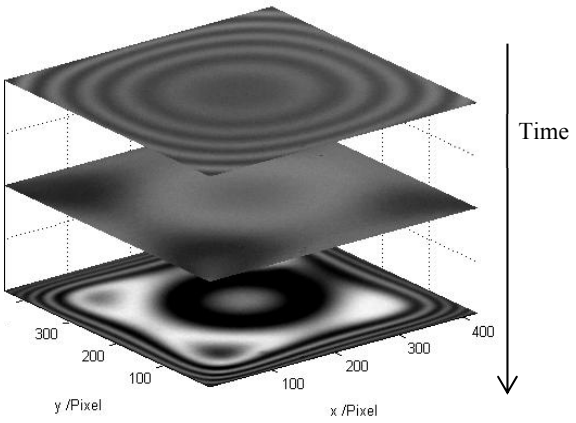

***Figure 9**. A slice plot showing the changing interferometry patterns and dimple formation from a fast drying methyl anisole drop. Images were recorded at 500 fps. The top image is at the beginning of drying and the bottom image near the end of drying.*

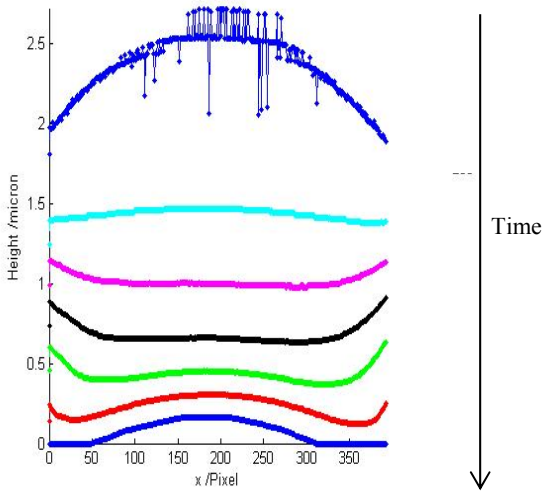

***Figure 10.** Changing profile of a drying methyl anisole drop with dimple formation in the later stages of drying and W- shaped final film profile. Time progresses from the top of the plot to the bottom. Total drying time was 10 s and the curves are equally spaced in time.*

The profile of the faster drying solvents could also be explained by the curvature in the film (figure 11). The negative Laplace pressure caused by the curvature resulted in fluid being sucked from the centre of the wells towards the walls. This capillary suction was present both in the slow and fast drying solvents. However in the faster drying solvents the evaporation was so rapid the capillary suction could not keep up with the drying and instead of taking fluid from the centre of the well it took fluid from the intermediate regions. Therefore the intermediate regions thinned more quickly than the centre of the drop to give a thicker fluid region at the centre and at the walls than in the intermediate regions. The dimpling of films is a phenomenon which has parallels in the dimple formation seen in the drainage of thin soap films [15,16].

***Figure 11**. A schematic showing how evaporation (blue arrows) and capillary suction (white arrows) thinned the film in intermediate regions and prevented capillary flows coming from the centre of the fluid.*

Thus far the solvents have been separated into fast and slow drying solvents. However, in reality the distinction was not so simple. The speed of drying of the solvent was greatly affected by a number of factors such as the relative distance between the nozzle and the substrate (which influences the relative vapour pressure). The most important factor in determining the profile of the drying film was the rate at which the solvent evaporated under the experimental conditions.

Conclusion

We have identified how drops dry on patterned substrates and which factors affect the profile of the film in the later stages of drying. Drying in patterned substrates is very different to the drying of a spherical cap drop with a pinned contact line on a flat substrate. With all solvents, the fluid began as a quasi-spherical cap sitting above the walls, before drying down to the level of the tops of the walls. Up to this point the flows seen were akin to those seen in the drying of a drop with an unconstrained contact line on a flat substrate. As the fluid dried down past the level of the walls it remained pinned at the tops of the walls. The speed of drying then determined whether a U- or W- shaped film profile developed.

The most important influence on uneven deposits when drops dry on patterned substrates was identified as capillary suction. Capillary action resulted from the negative Laplace pressure created by the curvature in the film when the drops pinned at the wall tops. This is a different mechanism to the cause of uneven deposits when drops dry on flat substrates. Controlling capillary flows within the walls is essential for obtaining uniform deposits.

References

[1] R. D. Deegan, O. Bakajin, T. F. Dupont, G. Huber, S. R. Nagel, T. A. Witten, "Capillary flow as the cause of ring stains from dried liquid drops", Nature., 389, 827 (1997).

[2] R. D. Deegan, O. Bakajin, T. F. Dupont, G. Huber, S. R. Nagel, T. A. Witten, "Contact line deposits in an evaporating drop", Phys. Rev. E., 62, 756 (2000).

[3] B. Derby, "Inkjet printing ceramics: From drops to solid", J. Eur. Ceram. Soc., 31, 2543 (2011).

[4] A. Teichler, Z. Shu, A. Wild, C. Bader, J. Nowotny, G. Kirchner, S. Harkema, J. Perelaer, U. S. Schubert, "Inkjet printing of chemically tailored light-emitting polymers", Eur. Polym. J., 49, 2186 (2013).

[5] S. H. Jung, J. J. Kim, H. J. Kim, "High performance injet printed phosphorescent organic light emitting diodes based on small molecules commonly used in vacuum processes", Thin Solid Films., 520, 6954 (2012).

[6] T. R. Hebner, D. Marcy, J. C. Sturm, C. C. Wu, "Fabrication of semiconductor devices using ink jet printing", Google Patents (2000).

[7] T. Hebner, C. Wu, D. Marcy, M. Lu, J. Sturm, "Ink-jet printing of doped polymers for organic light emitting devices", Appl. Phys. Lett., 72, 519 (1998).

[8] H. Hu, R. G. Larson, "Marangoni effect reverses coffee-ring deposits", J. Phys. Chem. B., 110, 7090 (2006).

[9] J. Park, J. Moon, "Control of colloidal particle deposit patterns within picoliter droplets ejected by ink-jet printing", Langmuir., 22, 3506 (2006).

[10] E. L. Talbot, L. Yang, A. Berson, C.D. Bain, "Control of the particle distribution in inkjet printing through an evaporation-driven sol-gel transition", ACS Applied Materials & Interfaces., 6, 9572 (2014).

[11] E. L. Talbot, H. N. Yow, L. Yang, A. Berson, S. R. Biggs, C. D. Bain, "Printing small dots from large drops", ACS Applied Materials & Interfaces., 7, 3782 (2015).

[12] V. R. Dugyala, M. G. Basavaraj, "Control over coffee-ring formation in evaporating liquid drops containing ellipsoids", Langmuir., 30, 8680 (2014).
[13] M. Singh, H. M. Haverinen, P. Dhagat, G. E. Jabbour, "Inkjet printing-process and its applications", Adv. Mater., 22, 673 (2010).
[14] J. N. Connor, R.G. Horn, "The influence of surface forces on thin film drainage between a fluid drop and a flat solid", Faraday Discuss., 123, 193 (2003).
[15] J. L. Joye, C. A. Miller, G. J. Hirasaki, "Dimple formation and behaviour during axisymmetrical foam film drainage", Langmuir., 8, 3083 (1992).
[16] L. Y. Clasohm, J. N. Connor, O. I. Vinogradova, R. G. Horn, "The "wimple": Rippled deformation of a fluid drop caused by hydrodynamic and surface forces during thin film drainage", Langmuir., 21, 8243 (2005).

Author Biography

Beth Kazmierski obtained her Masters in Chemistry at the University of Durham in 2013. She then remained at Durham to do her PhD within Prof. Colin Bain's research group, funded by an EPSRC iCASE award with Merck Chemicals. She is currently in the third year of her PhD which is looking into how drops dry on patterned substrates.

.